PARAMETRIC STUDY OF A HAND EXOSKELETON WITH A SOFT-RIGID MECHANISM

M. Fahrur Rozy Hentihu[1*], Dhafa[1], S. Syuhri[1], A. Triono[1], D. Djumhariyanto[1], R. D. Hidayatul Qoryah[1], H. Nurdiansyah[1] and K. Anam[1]

[1] Department of Mechanical Engineering, Universitas Jember, Jl. Kalimantan No. 37, Kampus Tegalboto-Jember, Indonesia

Corresponding Author's Email: fahrur.teknik@unej.ac.id

Article History: Received 27 November 2025; Revised 29 December 2025; Accepted 15 January 2026

ABSTRACT: *Stroke, a common cause of neurological deficits, frequently results in hand function impairment due to spasticity, necessitating rehabilitation intervention. Technology-based hand exoskeletons offer a potential solution for independent rehabilitation. This study aims to investigate crucial design parameters of a hand exoskeleton with a soft-rigid mechanism to optimize its performance, particularly in achieving a functional and safe range of motion for finger joints. A parametric study was conducted by evaluating a total of 12 design variations, differentiated by variations in segment thickness, shear gap height, and push plate material (Stainless Steel and Polycarbonate). The primary performance criteria were the ability to produce adequate bending angles at the Metacarpophalangeal (MCPJ), Proximal Interphalangeal (PIPJ), and Distal Interphalangeal (DIPJ) joints, without exceeding the material's allowable stress limit. The results indicated that two design variations (Design 10 and Design 12) exhibited optimal performance under safe stress conditions. Design 10 achieved bending angles of 142.64º (MCPJ), 140.53º (PIPJ), and 148.68º (DIPJ), while Design 12 reached angles of 141.75º (MCPJ), 148.43º (PIPJ), and 145.59º (DIPJ). This study successfully identified promising design parameter configurations for the development of effective and safe soft-rigid hand exoskeletons for post-stroke rehabilitation applications.*

KEYWORDS: *Stroke, Rehabilitation, Hand Exoskeleton, Soft-rigid Mechanism*

1.0 INTRODUCTION

A stroke, known scientifically as a cerebrovascular accident (CVA) [1], is characterized by the sudden onset of a neurological deficit. It is clinically defined as a rapidly developing syndrome of focal or global cerebral dysfunction, with symptoms lasting more than 24 hours or leading to death, originating from a vascular cause. The incidence of stroke increases significantly after the age of 40, establishing advanced age as a primary risk factor [2]. Strokes are broadly classified based on their underlying pathology. The most common type, ischemic stroke, results from the occlusion of a cerebral blood vessel, which obstructs blood flow and leads to ischemia—a critical shortage of oxygen and nutrients in the brain tissue supplied by the affected vessel. In contrast, a hemorrhagic stroke occurs when a cerebral artery ruptures, causing bleeding directly into or around the brain. This hemorrhage not only disrupts circulation but also increases intracranial pressure, causing direct damage to surrounding neural tissue [3].

Post-stroke spasticity can be mitigated through rehabilitative interventions designed to help patients regain lost bodily functions and activities, thereby maximizing their functional independence in activities of daily living (ADL) [4]. To optimize recovery outcomes, rehabilitation should be initiated as soon as the patient is medically stable. This process leverages the brain's capacity for neuroplasticity, allowing it to relearn or form new pathways to compensate for abilities compromised by the stroke. Rehabilitation methods are broadly categorized into two types: active rehabilitation, which requires the patient to perform movements using their own muscular effort, and passive rehabilitation, where movement is facilitated by an external force, such as a physiotherapist or a mechanical device [5].

The use of robotic hand exoskeletons in post-stroke rehabilitation serves as an alternative for conducting regular, independent therapy while also helping to restore the functional abilities of the hand [6]. These robotic devices are vital for stroke patients seeking to restore nerve function and the ability to grasp objects normally and independently. A robotic hand exoskeleton is a mechatronic development in the field of robotics; these systems are developed for applications such as human power augmentation, rehabilitation robotics, assistive technology, and haptic interaction in virtual reality. Actuators integrated into the exoskeleton enable the structure to mimic human finger movements, including flexion, extension, and adduction. In the healthcare context, the robotic hand exoskeleton represents a technological development that applies principles of biological adaptation to the environment [7]. There are two primary construction types: the 'precision grip,' which tends to have a complex mechanical design, making it less practical and heavier to use despite its utility. In contrast, the 'power grip' features a simpler construction, is easier to use, and, in addition to rehabilitation, can assist with daily activities such as grasping objects to support the user's independence [8].

The term 'Soft-Rigid' refers to a type of structure that combines properties of both flexibility and stiffness. In this context, "Soft" denotes the structure's flexibility or its capacity to undergo deformation and change shape, whereas "Rigid" refers to its ability to maintain its form and relative stiffness [9].

This study will focus on the design parameter optimization of a rigid hand exoskeleton structure. The parameters to be varied in this research include the sliding slot height of the rigid segment's driving plate, the dimensions of the rigid segment, and the driving plate material. Each resulting design variation will be subjected to a static structural simulation to evaluate its performance on the index finger phalanx during flexion motion.

2.0 RESEARCH METHODOLOGY

Data collection for this study is conducted through a literature review combined with the use of design and structural analysis software. The required data will be processed and used in calculations and analysis to determine performance metrics, namely maximum stress and permissible deformation. To support this research, several tools and materials are utilized, including a computer system equipped with Solidworks for 3D design and Ansys for analysis. The research variables consist of independent, dependent, and control variables. The independent variables include variations in the dimensions of the rigid segment, the height of the sliding slot, and the driving plate.

The complete representation of the design is presented in Figure 1. This illustration provides a detailed depiction of the rigid segment's thickness, the dimensional specification of the thrust plate, and the measured height of the shear gap.

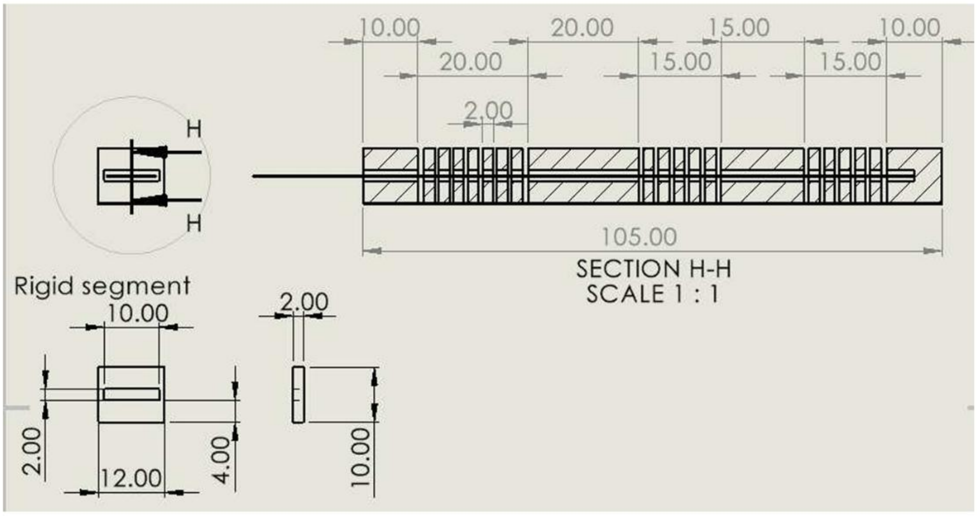

Figure 1. Soft Rigid Hand Exoskeleton Design

Based on the design, it is possible to generate variations in the thickness of each rigid segment, the dimensional parameters of the thrust plate, and the height of the shear gap. These variations are comprehensively presented in Table 1.

Table 1. Soft Rigid Hand Exoskeleton Design Variations Mechanism

Design	Rigid segment thickness (mm)	Thickness of the thrust plate (mm)	Shear Gap Height (mm)
1	2	0.3	4
2	2	0.3	7
3	2	0.5	4
4	2	0.5	7
5	4	0.3	4
6	4	0.3	7
7	4	0.5	4
8	4	0.5	7
9	2	1*	4
10	2	1*	7
11	4	1*	4
12	4	1*	7

** . Material Polycarbonate*

The meshing outcome generated for the simulation, derived from the previously established design, is presented in Figure 2. This figure illustrates the discretization of the model's geometry into finite elements, enabling precise numerical analysis. The mesh configuration was developed to ensure an optimal balance between computational efficiency and accuracy, with element sizes and distribution tailored to capture critical geometric features and regions of expected high stress gradients.

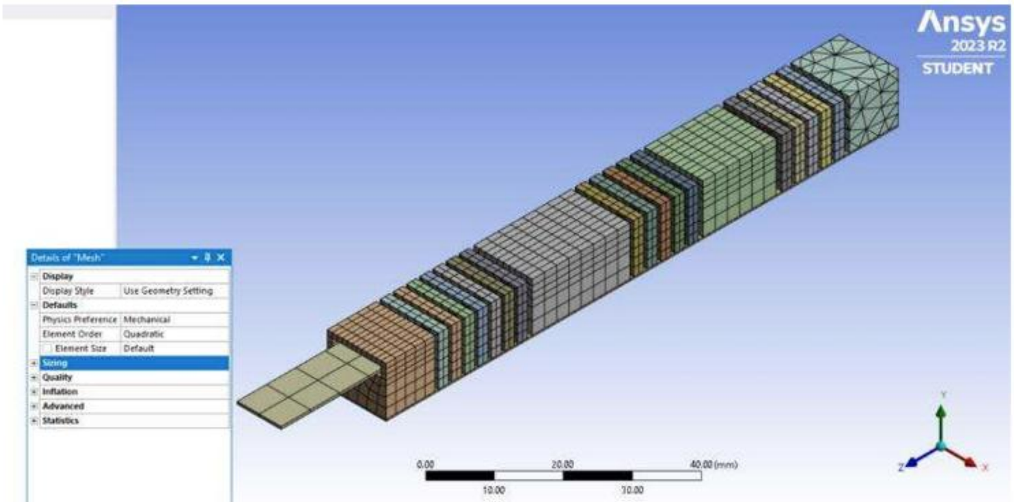

Figure 2. Meshing

The dependent variables focus on the maximum stress and total deformation, which are then compared to the allowable stress based on a safety factor of 1.5. Meanwhile, the established control variables are the materials used—namely PLA, SS304, and Polycarbonate—as well as the fixed support points chosen for the simulation process.

Allowable stress is the maximum stress that any part of a structure is permitted to experience, as determined by the safety factor [10]. As long as the maximum stress does not exceed the allowable stress, the structure is considered safe. Conversely, if the maximum stress is greater than the allowable stress, the structure is deemed unsafe. The allowable stress can be calculated using the following equation:

$$\sigma_{\ Allowable} = \frac{\sigma_y}{n} \tag{1}$$

where:
σ_{izin} = Allowable stress (MPa)
σ_y = Tensile yield strenght (MPa)
n = Safety Factor

Therefore, the primary performance criteria for this study were the ability to produce adequate bending angles at the Metacarpophalangeal Joint (MCPJ), Proximal Interphalangeal Joint (PIPJ) [11], and Distal Interphalangeal Joint (DIPJ) [12], while ensuring the maximum Von Mises stress did not exceed the material's calculated allowable stress.

Table 2. *Material Properties*

Unit	Material		
	PLA	Polycarbonate	SS 304
Yield (MPa)	41.9	65.9	210
UTS (MPa)	58.9	62.7	500
Modulus Young (GPa)	2.35	2.31	185
Density (gr/cc)	1.3	1.2	8
Poisson ratio	0.35	0.353	0.27
Allowable stress (MPa)	27.93	43.93	140

ISSN 2180-1053 e-ISSN 2289-8123 Vol.18 No.1

In this simulation, no external force was directly applied; instead, a displacement was prescribed. From Figure 3, it can be observed that the plate was pushed forward by 15 mm, causing the finger to curl. This curling motion generated a curved deformation profile, which in turn induced a significant deflection. The resulting deflection led to elevated stress levels within the plate.

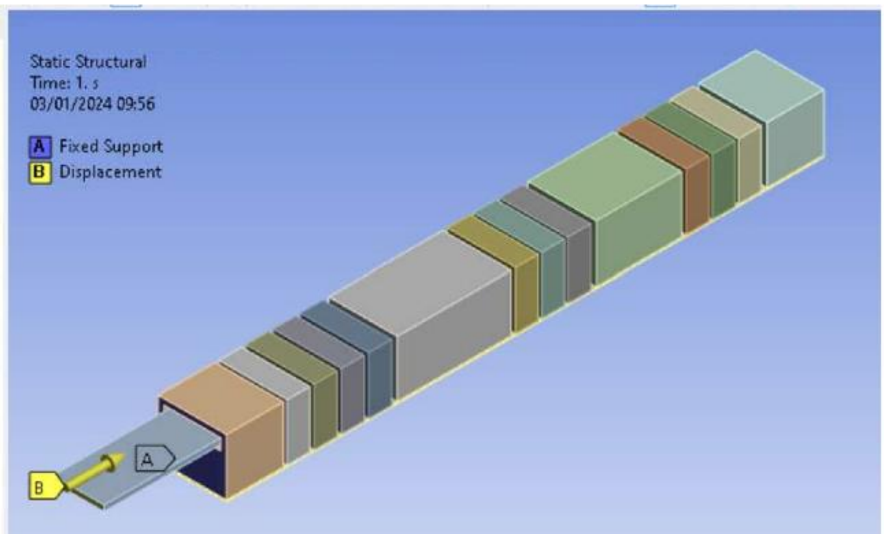

Figure 3. Prescribed displacement

3.0 RESULT AND DISCUSSION

The overall simulation results are shown in Figure 4. For the driving plate, the highest maximum Von Mises Stress was found in designs 1-8, all of which exceeded the 140 MPa allowable stress for SS304. The greatest stress value was 299.62 MPa in design 2, while the smallest was 226.25 MPa in design 1.

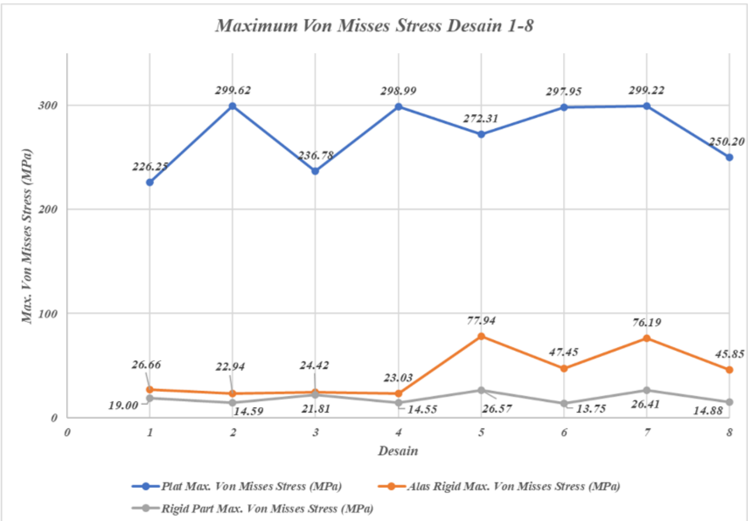

Figure 4. Graphic *Max. Von Misses Stress* design 1-8

Furthermore, the highest maximum Von Mises Stress on the base of the rigid segment was found in design 5 with a value of 77.94 MPa, while the lowest value was found in design 2, with a value of 222.94 MPa. In designs 5-8, the maximum Von Mises Stress on the base of the rigid segment exceeded the 43.93 MPa allowable stress for Polycarbonate, rendering them unsuitable.

Based on the analysis of the various materials considered in the proposed design, it was observed that all options exhibit stress levels within their respective allowable limits under static conditions. However, the stress distribution curve generated after dynamic motion indicates localized stress concentrations that exceed the allowable stress threshold. Consequently, it is recommended to employ alternative materials with higher allowable stress capacities, such as AISI 1045 steel, to ensure structural integrity and improve the design's performance under dynamic loading.

For the rigid segment itself, the highest maximum Von Mises Stress was observed in design 5 at 26.57 MPa, and the lowest was in design 6 at 13.75 MPa. Across all designs, the maximum Von Mises Stress on the rigid segment component remained below its allowable stress.

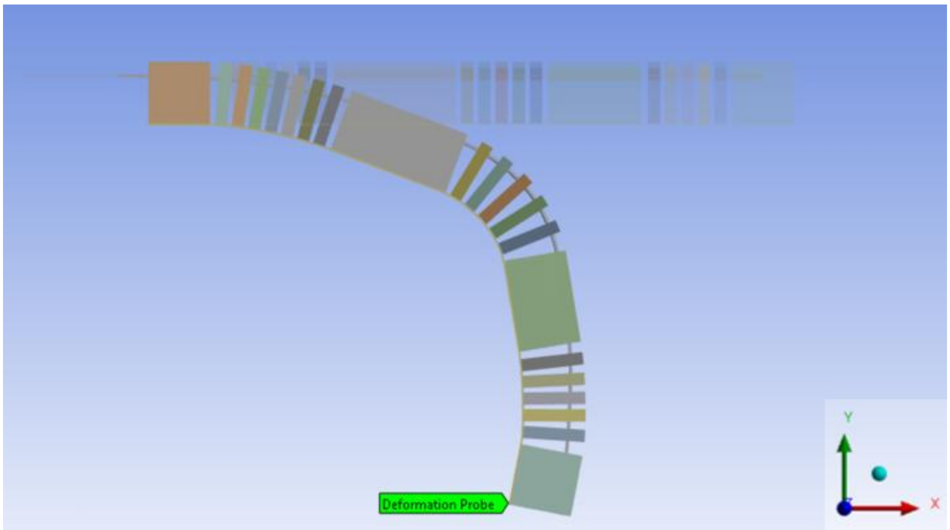

Figure 5. Probe *Deformation* Position

Table 3 Deformation Simulation Results and Displacement Probe of 304 Stainless Steel Pusher Plate Design

Design	Total Deformation (mm)	Displacement X axis (mm)	Displacement Y axis (mm)
1	124.38	-98.99	-73.33
2	82.29	-46.46	-51.56
3	125.57	-96.67	-66.36
4	82.30	-46.56	-61.55
5	110.45	-73.80	-66.87
6	91.33	-48.07	-70.53
7	113.08	-76.76	-67.54
8	90.81	-47.75	-70.22

In Table 3 above, the results of the total deformation or the largest geometric changes are shown in design 3 with a total deformation of 125.57 mm with a displacement of the end of the rigid segment of 96.67 mm on the x-axis and -66.36 mm on the y-axis. The overall simulation results for designs 9-12 are shown in Figure 6 above. For the driving plate, the highest maximum Von Mises Stress was found in design 11 at 57.72 MPa, while the smallest was in design 10 at 226.25 MPa.

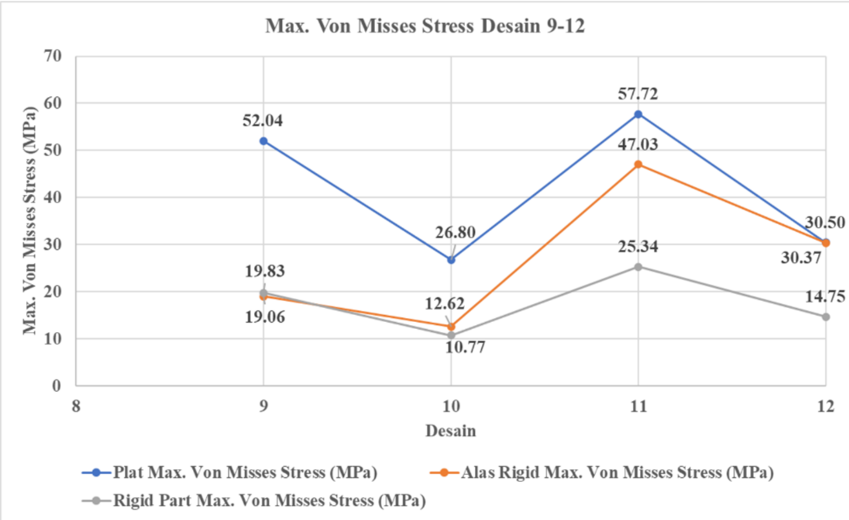

Figure 6. Graphic *Max. Von Misses Stress* design 9-12

Next, the highest maximum Von Mises Stress on the base of the rigid segment was found in design 11 with a value of 47.03 MPa, and the lowest value was in design 10 at 12.62 MPa. The maximum Von Mises Stress on the rigid segment itself was highest in design 11 at 25.34 MPa and lowest in design 10 at 10.77 MPa. For the rigid segment component, all designs had a maximum Von Mises Stress that was below their allowable stress.

Table 4 Deformation Simulation Results and Displacement Probe 304 Stainless Steel Pusher Plate Design

Design	Total Deformation (mm)	Displacement X axis (mm)	Displacement Y axis (mm)
9	123.92	-90.71	-72.07
10	93.32	-51.92	-69.72
11	116.78	-81.39	-70.33
12	93.00	-48.58	-70.28

Based on the simulation results shown in Table 4, it is observed that the largest total deformation occurred in design 10, with a value of 123.92 mm, featuring axial deformations of -90.71 mm on the x-axis and -72.07 mm on the y-axis. The largest total deformation was also found in designs 9 and 11, which used a sliding slot height of 4 mm. Therefore, it can be concluded that the sliding slot height has a significant influence on the total deformation produced in the simulation of the soft-rigid mechanism hand exoskeleton design with a 1 mm polycarbonate driving plate.

Based on Figure 7, it can be seen that the bending angles for designs 10 and 12 are smaller at the DIPJ and PIPJ compared to the robotic hand developed by Nazari [13]. However, for the MCPJ section, designs 10 and 12 have a larger bending angle. This larger MCPJ bending angle in designs 10 and 12 is caused by the sliding slot height, which increases the radius of curvature that the hand exoskeleton system can form. This wider radius is an effect of the smaller angle between the rigid segments.

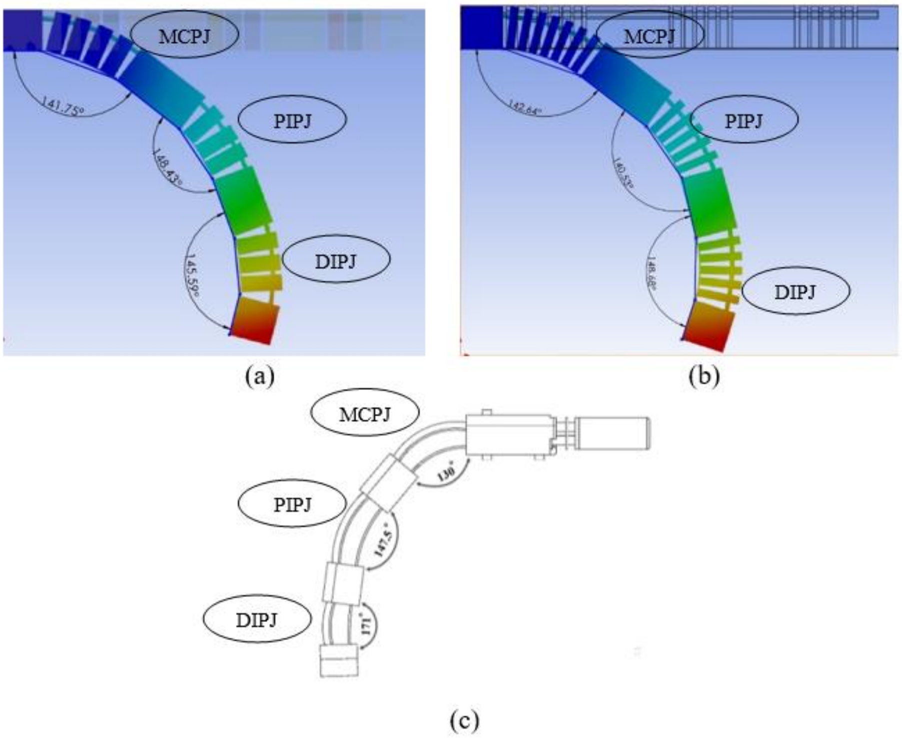

Figure 7. Bending Angle (a) Design 10; (b) Design 12; (c) Nazari Design [13]

4.0 CONCLUSION

1. The simulation results for the designs using a Stainless Steel 304 driving plate showed poor performance, with all designs experiencing failure in the plate section. This occurred because the resulting maximum Von Mises Stress was greater than the predetermined allowable stress for Stainless Steel 304. Among designs 1 through 8, the one with the best performance was design 1, which had a maximum Von Mises Stress of 226.25 MPa on the plate, 26.66 MPa on the base, and 19.00 MPa on the rigid segment.

2. The largest total deformation among designs 1-8 was found in design 2, with a value of 125.57 mm. This included an x-axis displacement of 96.67 mm and a y-axis displacement of 66.36 mm. Design 3 also exhibited large deformation, which was attributed to its 4 mm sliding slot height and 2 mm rigid segment thickness, causing the radius of curvature of the hand exoskeleton system to become smaller.

3. In conclusion, AISI 1045 steel is identified as the most suitable material for the proposed design.

4. The largest total deformation among designs 1-8 was found in design 2, with a value of 125.57 mm. This included a displacement of 96.67 mm on the x-axis and 66.36 mm on the y-axis. Design 3 also exhibited large deformation, which was attributed to its 4 mm sliding slot height and 2 mm rigid segment thickness, causing the radius of curvature of the hand exoskeleton system to become smaller. The simulation results for the designs with a 1 mm Polycarbonate driving plate showed poor outcomes for designs 9 and 11. These designs failed in the plate section because the maximum Von Mises Stress produced was greater

than the predetermined allowable stress for Polycarbonate (with a value of 52.04 MPa). Furthermore, design 11 experienced failure in the driving plate, the base, and the rigid segment. In contrast, designs 10 and 12 performed well, as their Von Mises Stress values remained below the allowable stress.

5. The largest total deformation among designs 9-12 was produced by design 9. Design 9 had the greatest deformation because it utilized a sliding slot with a height of 4 mm and a rigid segment thickness of 2 mm, which caused the radius of curvature of the hand exoskeleton system to become smaller.

6. Based on the overall simulation results, designs 10 and 12 were found to be suitable for application as a hand exoskeleton.

7. The bending angle measurements for design 10 resulted in values of 142.64º at the MCPJ, 140.53º at the PIPJ, and 148.68º at the DIPJ. The measurements for design 12 showed values of 141.75º at the MCPJ, 148.43º at the PIPJ, and 145.59º at the DIPJ. The magnitude of the bending angles produced by designs 10 and 12 successfully addresses the problems identified by [13] by achieving smaller bending angles at the DIPJ and PIPJ.

ACKNOWLEDGEMENT

This research is financially supported by Undergrad Thesis Reworking Grant, Institute for Research and Community Service, Universitas Jember.

REFERENCES

[1] R. Pandit, M. Mathews, and S. Sangle, "Assessment of neurological deficit among cerebrovascular accident patient in selected hospital", *International Journal Health Sci Res*, vol. 7, pp. 221–6, 2017.

[2] L. Nasution, "Stroke Non Hemoragik pada Laki-Laki Usia 65 Tahun", *Medula*, vol.1, 2013.

[3] D. Kuswanto, I. Iskandriawan, P. S. Mahardhika, " Power Grip Exoskeleton Design as Rehabilitation Devices for Post-Stroke Survivors", *Conference: 2018 1st International Conference on Bioinformatics, Biotechnology, and Biomedical Engineering (BioMIC) - Bioinformatics and Biomedical Engineering*, 2018.

[4] C. Stinear, C. E. Lang, and S. Zeiler,"Advances and challenges in stroke rehabilitation", *Lancet Neurol*, vol. 19, no.4, pp. 348-360, 2020.

[5] D. Popov, I. Gaponov, I., and J. H. Ryu, "Portable exoskeleton glove with soft structure for hand assistance in activities of daily living" *IEEE/ASME Transactions on Mechatronics*, vol. 22, no. 2, 865–875, 2017.

[6] D. Kuswanto, B. Iskandriawan, and P. S. Mahardhika, "Power Grip Exoskeleton Design as Rehabilitation Devices for Post-Stroke Survivors", *Proceedings, 2018 1st*

International Conference on Bioinformatics, Biotechnology, and Biomedical Engineering : 19-20 October 2018 Eastparc Hotel, Yogyakarta, Indonesia.

[7] O. Sandoval-Gonzalez, J. Jacinto-Villegas, I. Herrera-Aguilar, O. Portillo-Rodiguez, P. Tripicchio, M. Hernandez-Ramos, A. Flores-Cuautle, and C. Avizzano, "Design and Development of a Hand Exoskeleton Robot for Active and Passive Rehabilitation", *International Journal of Advanced Robotic Systems*, 2016, https://doi.org/10.5772/62404.

[8] P. S. Mahardika, "*Desain Power-Grip Exoskeleton sebagai Alat Bantu Rehabilitasi Pasien Pasca-Strok*", Institut Teknologi Sepuluh November, 2018.

[9] R. Bimo, P. Sukoco, W. Hendroprasetyo, A. Putra, D. Septia, and H. Sujiatanti, "Analisis Tegangan pada Penegar Wrang Pelat Akibat Kemiringan Penegar Wrang Pelat", *Jurnal Teknik ITS*, vol.*7*, no.2, 2018.

[10] L. Lin, F. Zhang, L. Yang, and Y. Fu, "Design and modeling of a hybrid soft-rigid hand exoskeleton for poststroke rehabilitation", *International Journal of Mechanical Sciences*, vol. *212*, 2021.

[11] W. H. Bowers, J. W. Wolf Jr, J. L. Nehil, and S. Bittinger, "The proximal interphalangeal joint volar plate. I. An anatomical and biomechanical study", *The Journal of hand surgery*, vol. 5, no.1, pp. 79–88, 2018.

[12] A. Roda-Sales, J. L. Sancho-Bru and M. Vergara, "Studying kinematic linkage of finger joints: estimation of kinematics of distal interphalangeal joints during manipulation", *Peer J*, vol. 10, e14051, 2022.

[13] V. Nazari, M. Pouladian, Y. P. Zheng, and M. Alam, "A compact and lightweight rehabilitative exoskeleton to restore grasping functions for people with hand paralysis", *Sensors*, vol. 21, no.20, 2021.